Modelling Analysis of Pre-stress Effect on Upper Critical Magnetic Field and Critical Current of Nb_3Sn Composite Wire(High Field Superconductors)

Modelling Analysis of Pre-stress Effect on Upper Critical Magnetic Field and Critical Current of Nb_3Sn Composite Wire*

S. Ochiai[a], S. Nishino[a], M. Hojo[a], K. Osamura[a] and K. Watanabe[b]

[a] Faculty of Engineerng, Kyoto University, Sakyo-ku, Kyoto 606-01, Japan.
[b] Institute for Materials Research, Tohoku University, Sendai 980-77, Japan.

An analytical model to describe the variations of the upper critical magnetic field and critical current at 4.2K of the superconducting multifilamentary Nb_3Sn composite wire caused by the application of pre-stress at room tempearture was presented and applied to experimental results. Main results are summarized as follows. (1)The variations of the upper critical magnetic field and critical current could be described well as a function of pre-stress by combining the Ekin's scaling law with the elastic/plastic mechanical calculation. (2)It was demonstrated experimentally and theoretically that the upper magnetic filed and critical current can be improved by the pre-stressing treatment through the control of residual strain of Nb_3Sn. (3)The strength distribution of the Nb_3Sn filaments was estimated for the first time by extracting the influence of breakage of Nb_3Sn filaments from the change in critical current of pre-stressed composite. (4)The procedure to predict the relation between critical current at 4.2K and pre-stress at room temperature for engineering-scale long samples was presented based on the present model. An example of the application indicated that the permissible overall pre-stress on composite, below which all Nb_3Sn filaments transport current without breakage, is reduced by ≈20 % for long specimens of 300m in comparison with that for the short specimens of 25mm, while the average strength of Nb_3Sn for 300 m is reduced by ≈60 % from that for 25mm.

1. Introduction

During fabrication and/or service, mechanical and electromagnetic forces are exerted on superconducting composite wire, whcich affect on superconducting properties. In case of Nb_3Sn superconducting composite wire, much effort has been made to clarify the influence of stress of Nb_3Sn on the critical current I_c, the critical temperature T_c and the upper critical magnetic field H_{c2}[1-12]. It has been confirmed that I_c, T_c and H_{c2} show their maximum values in the stress-free state of Nb_3Sn and decrease with increasing compressive and tensile stresses. Therefore the compressive residual stress in Nb_3Sn introduced by cooling from heat-treatment temperature reduces the values of I_c, T_c and H_{c2} in comparison with those in the stress-free state.

From the view-point of the control of residual strain, the authors[13-15] have demonstrated that the pre-stressing treatment (stressing followed by releasing) on composite samples at room temperature is effective; the critical current at 4.2K increases, reaching maximum at zero strain of Nb_3Sn at 4.2K and then decreases with increasing applied stress, which can be described by the variation of the strain of Nb_3Sn calculated by the elastic/plastic mechancal calculation in combination with Ekin's scaling law[10-12]. However, the influence of the breakage of the Nb_3Sn filaments,

which reduces critical current seriously, has not been clarified at that time. Thus the application of this analysis has been limited only to the relatively low pre-stress range.

Recently, the authors have developed a method to evaluate the strength distribution of Nb_3Sn from the analysis of the variation of critical current of the pre-stressed composite wires[16,17]. Modification of this method made it possible to predict the variation of critical current of engineering-scale long pre-stressed composite wire[18]. Then it becomes possible to describe and predict quantitatively the pre-stress effect on upper critical magnetic field and critical current for any pre-stress and length of samples. The present paper summarizes this analytical approch and the results of application.

2. Analytical Procedure to Estimate the Influence of Pre-stress on Upper Critical Magnetic Field and Critical Current

The flow chart to estimate the influence of the pre-stress on the upper critical magnetic field and critical current, to estimate the strength distribution of Nb_3Sn, and to predict the length-dependence of the critical current of the pre-stressed composite wire, is presented in Fig.1. The background and detailed procedure are as follows.
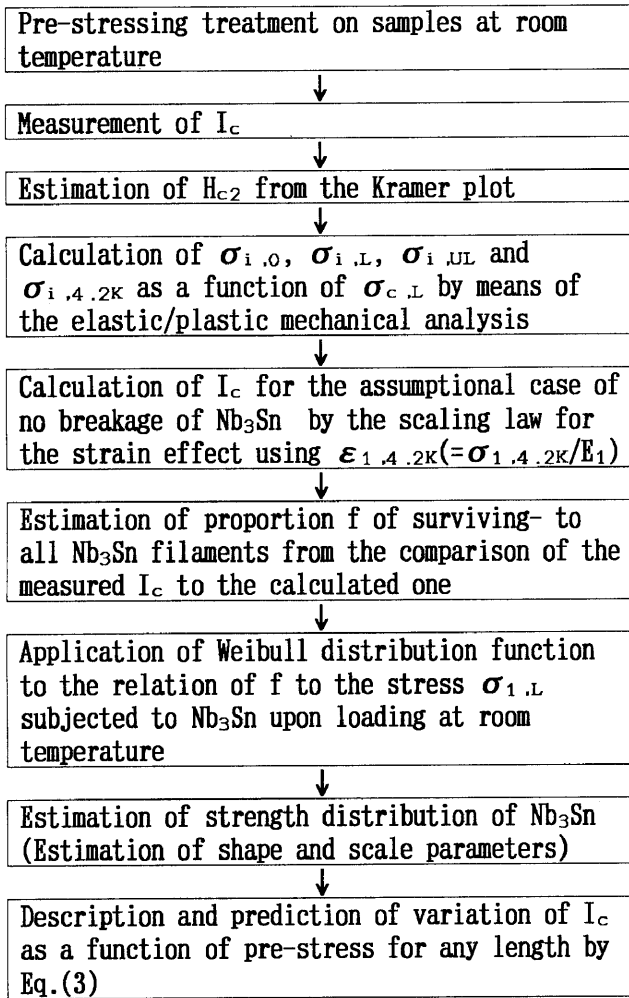
Pre-stressing treatment on samples at room temperature

↓

Measurement of I_c

↓

Estimation of H_{c2} from the Kramer plot

↓

Calculation of $\sigma_{i,0}$, $\sigma_{i,L}$, $\sigma_{i,UL}$ and $\sigma_{i,4.2K}$ as a function of $\sigma_{c,L}$ by means of the elastic/plastic mechanical analysis

↓

Calculation of I_c for the assumptional case of no breakage of Nb_3Sn by the scaling law for the strain effect using $\varepsilon_{1,4.2K}(=\sigma_{1,4.2K}/E_1)$

↓

Estimation of proportion f of surviving- to all Nb_3Sn filaments from the comparison of the measured I_c to the calculated one

↓

Application of Weibull distribution function to the relation of f to the stress $\sigma_{1,L}$ subjected to Nb_3Sn upon loading at room temperature

↓

Estimation of strength distribution of Nb_3Sn (Estimation of shape and scale parameters)

↓

Description and prediction of variation of I_c as a function of pre-stress for any length by Eq.(3)

Figure 1   Flow chart for estimation of the relation of the pre-stress applied to composite wire $\sigma_{c,L}$ to upper critical magnetic field H_{c2} and critical current I_c. $\sigma_{i,L}$ is the stress exerted on the constitituent i(i=1 to 4 correspond to Nb_3Sn, Nb, Cu-Sn and Cu, respectively) upon stressing of composite to $\sigma_{c,L}$. $\sigma_{i,0}$ and $\sigma_{i,UL}$ are the residual stresses at room temperature before and after the pre-stressing treatment, respectively, and $\sigma_{i,4.2K}$ is the residual stress at 4.2K.

(A)Scaling law

Figure 2 shows the strain effect on the upper critical magnetic field H_{c2} and critical current I_c at 4.2K. H_{c2}- and I_c-values are very sensitive to the strain of Nb_3Sn; they become maximum(H_{c2m} and I_{cm}) in the strain-free state of Nb_3Sn, and decrease with increasing compressive and tensile stresses. The strain effect on H_{c2} is empirically given as a function of the strain of Nb_3Sn at 4.2K, $\varepsilon_{1,4.2K}$, in the form[10-12]

$$H_{c2}/H_{c2m}=1-a|\varepsilon_{1,4.2K}|^u, \qquad (1)$$

where a is a constant equal to 900 for compressive strain(negative $\varepsilon_{1,4.2K}$) and 1250 for tensile strain(positive $\varepsilon_{1,4.2K}$), and u is also the constant given by 1.7.
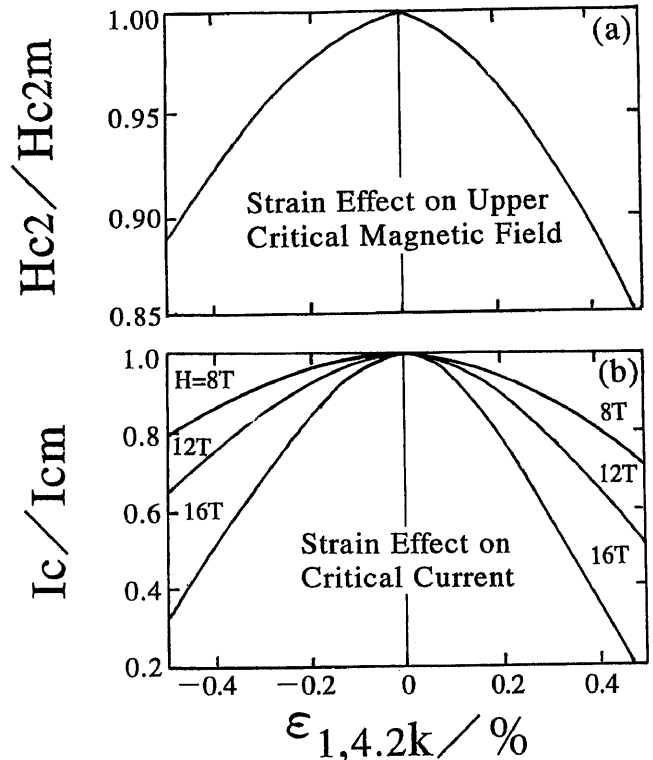

Figure 2   Ekin's scaling law of the strain effects (a)on the upper critical magnetic field H_{c2} given by Eq.(1) and (b)on the critical current I_c of Nb_3Sn given by Eq.(2), in which H_{c2} and I_c are normalized with respect to the values at zero strain, H_{c2m} and I_{cm}, respectively. In this calculation of I_c/I_{cm}, H_{c2m} is taken to be 21T as an example.
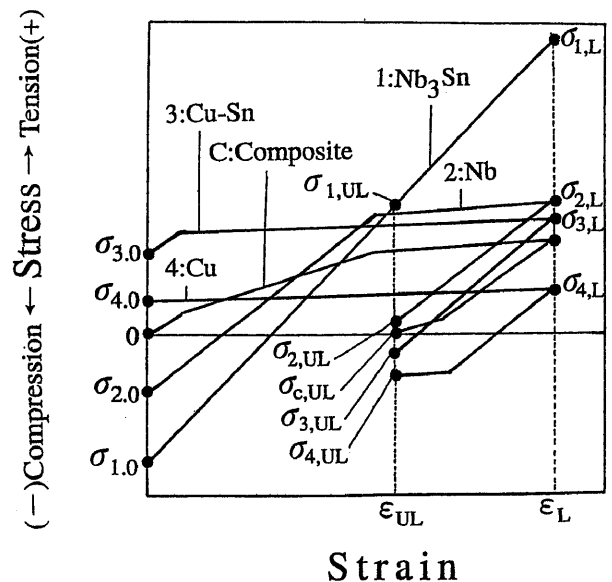

Strain

Figure 3   Schematic drawing of the stress-strain curves of the composite(noted as C) and the constituents of Nb_3Sn(1), niobium(2), bronze(3) and copper(4) during pre-stressing treatment (stressing followed by releasing). $\sigma_{i,0}$, $\sigma_{i,L}$ and $\sigma_{i,UL}$(i=1 to 4) show the residual stress introduced by the cooling from heat-treatment- to room temperature, the exerted stress at the applied stress on composite $\sigma_{c,L}$, and the residual stress after pre-stressing treatment, respectively.

Similarly, the relation of the relative current I_c/I_{cm} to the strain of Nb_3Sn can be expressed by the Ekin's scaling low[10-12] given by

$$I_c/I_{cm}=(H_{c2}/H_{c2m})^{1/2}\{(1-H/H_{c2})/(1-H/H_{c2m})\}^2. \quad (2)$$

(B)Control of residual strain of Nb_3Sn by pre-stressing treatment at room temperature

When composite samples are cooled down from the heat-treatment temperature, compressive stresses are exerted on the Nb_3Sn and niobium, and tensile ones on the bronze and copper due to the difference in thermal expansion among the constituents. Therefore, the I_c and H_{c2} are never higher than I_{cm} and H_{c2m}, respectively. Figure 3 shows the schematic representation of the stress-strain curves of the composite as a whole(noted as C) and the constituents of $Nb_3Sn(1)$, niobium(2), bronze(3) and copper(4) during the pre-stressing treatment. Upon stressing (loading of samples), the stress of composite increases from zero to $\sigma_{c,L}$ and the stress of each constituent increases from the residual stress $\sigma_{i,0}$ to $\sigma_{i,L}$ where the subscripts i=1 to 4 refer to Nb_3Sn, niobium, bronze and copper, respectively, and the

subscript L to loading. When the applied stress is released by unloading, the stress on composite becomes zero($\sigma_{c,UL}$) and the residual stress of each constituent becomes $\sigma_{i,UL}$ where the subscript UL refers to unloading. Consequently, the residual stress of each constituent is changed from $\sigma_{i,0}$ to $\sigma_{i,UL}$ by the pre-stressing treatment. By changing the pre-stress level($\sigma_{c,L}$) widely, the residual stress of Nb_3Sn after pre-stressing treatment can be changed extensively. In this way, the strain of Nb_3Sn can be controlled by this treatment, which makes it possible to improve the superconducting property[13-15].

Figures 4(a) to (c) show an example of the calculation of the variations of the stress exerted on each constituent (a)upon stressing at room temperature ($\sigma_{i,L}$), (b)after pre-stressing at room temperature ($\sigma_{i,UL}$) and (c)at 4.2K($\sigma_{i,4.2K}$) as a function of $\sigma_{c,L}$. The specification of the sample used in this calculation is the same as that of the sample used in the present experiment, which will be shown later in detail. Once the relation of $\varepsilon_{1,4.2K}(=\sigma_{1,4.2K}/E_1$ where E_1 is the Young's modulus of Nb_3Sn) to $\sigma_{c,L}$ is calculated, the effect of pre-stress treatment on H_{c2}/H_{c2m} can be predicted by substituting the calculated values of $\varepsilon_{1,4.2K}$ into Eq.(1), as shown in (d). Then using the
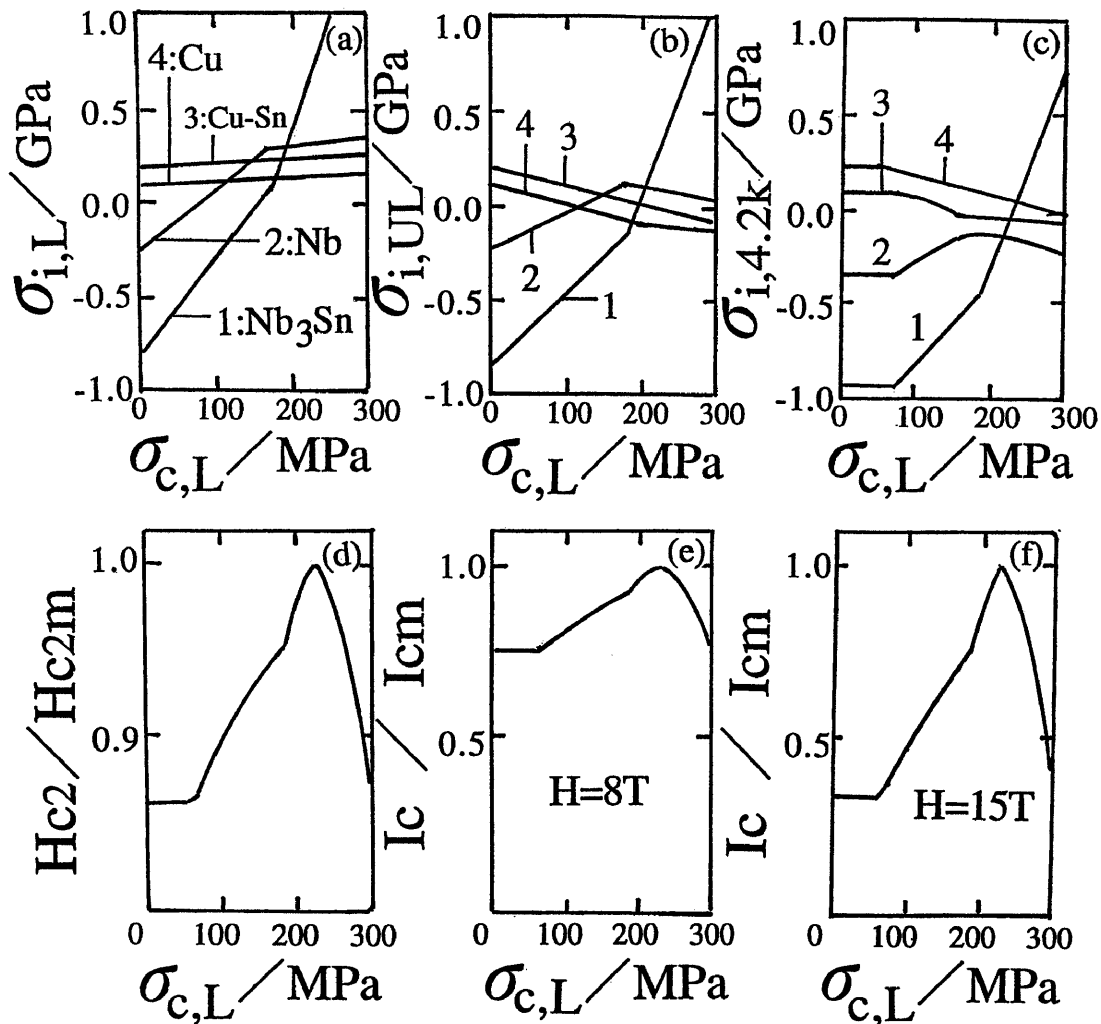

Figure 4 An example of the calculation result of the variations of (a)$\sigma_{i,L}$(i=1 to 4), (b)$\sigma_{i,UL}$(i=1 to 4), (c)$\sigma_{1,4.2K}$,(d)H_{c2}/H_{c2m}, (e)I_c/I_{cm} for H=8T and (f)I_c/I_{cm} for H=15T as a function of $\sigma_{c,L}$. The H_{c2m} for calculation of I_c/I_{cm}(e and f) is assumed to be 21T in this example.

Figure 5 Appearance of Nb_3Sn pre-stressed up to $\sigma_{c,L}=$ 258MPa. The co-existence of the broken and unbroken Nb_3Sn indicates that the strength of each Nb_3Sn filament is different.

relation of H_{c2} to $\sigma_{c,L}$, the relation of I_c to $\sigma_{c,L}$ can be calculated by Eq.(2) for a given H_{c2m}-value, as shown in (e) and (f).

On the other hand, when the exerted stress on Nb_3Sn exceeds the tensile strength of Nb_3Sn, the Nb_3Sn is broken, resulting in serious reduction in critical current[13-15]. As a large number of Nb_3Sn filaments are embedded in composite wire, weaker Nb_3Sn are broken prior to stronger ones as shown in Fig.5. For a description of the pre-stressing effect on critical current for a wide range of $\sigma_{c,L}$, a quantitative estimation of the strength distribution of Nb_3Sn is needed.

(C)Estimation of strength distribution of Nb_3Sn

The critical current of the composite samples is transported only by the surviving(unbroken) Nb_3Sn filaments. The proportion of the surviving- to all filaments, f, varies from unity, at which no breakage of Nb_3Sn occurs(all filaments transport current) to zero, at which all Nb_3Sn filaments are broken(no filaments transport current). Thus the scaling law of Ekin[10-12] modified as to describe the influence of breakage of Nb_3Sn will be given by[16]

$$I_c=fI_{cm}(H_{c2}/H_{c2m})^{1/2}\{(1-H/H_{c2})/(1-H/H_{c2m})\}^2. \quad (3)$$

For evaluation of the f-value for each specimen, first the I_c-H relation is calculated for the assumptional case of f=1 by substituting the measured values of I_{cm}, H_{c2} and H_{c2m} into Eq.(3). Then only the f-value is varied in Eq.(3) and a f-value fitting best to experimental I_c-H relation is chosen.

For description of the strength distribution of various metals and ceramics, two-parameter Weibull distribution function[19] has widely been employed. According to this distribution function, the cumulative

probability of failure F at stress $\sigma_{1,L}$ for the Nb_3Sn of a length L is given by

$$F=1-f=1-\exp\{-(L/L_0)(\sigma_{1,L}/\sigma_0)^m\}, \quad (4)$$

where m and σ_0 are shape and scale parameters, respectively, and L_0 is the standard length (taken to be 1 m(meter) in the present work). The m-value is a measure of the scatter; the smaller the m-value, the larger becomes the scatter. To estimate the shape(m) and scale(σ_0) parameters, Eq.(4) is modified to

$$\ln\ln(1/f)=m[\ln\{(\sigma_{1,L}/\sigma_0)\}]+\ln(L/L_0). \quad (5)$$

Then the values of m and σ_0 are obtained from the slope and intersection of plot of $\ln\ln(1/f)$ against $\ln(\sigma_{1,L})$ (Weibull plot). The average strength of Nb_3Sn, $\sigma_{1,F}$(ave), is given by

$$\sigma_{1,F}(\text{ave})=\sigma_0(L_0/L)^{1/m}\Gamma(1+1/m), \quad (6)$$

where Γ is the gammma function.

(D)Prediction of variation of critical current of pre-stressed composite for any length

Once the shape- and scale parameters of the Weibull distribution function are known, the strength distribution of Nb_3Sn can be calculated for any length by Eq.(4). Substituting f calculated by Eq.(4), the experimentally measured H_{c2m} and I_{cm} for short samples, $\varepsilon_{1,4.2K}$ calculated by elastic/plastic mechanics, and H_{c2} calculated by Eq.(1) into Eq.(3), we can predict variation of I_c as a function of $\sigma_{c,L}$ for any length.

3. Experimental Procedure

Samples of multifilamentary bronze-processed Nb_3Sn composite wire with an overall diameter of 0.59mm, bronze ratio of 0.445 and copper ratio of 2, composed of 745 niobium filaments in a Cu-7.4at% Sn alloy, surrounded with a niobium barrier and then copper as a stabilizer, were heat-treated at 973K for 43ks for the formation of Nb_3Sn. The volume fraction of Nb_3Sn was 0.07 and the Sn concentration in the bronze was 4.8at% in the present specimens.

The specimens were stresssed at room temperature up to various stress levels(0-300 MPa) at a strain rate of 6.7×10^{-4}/s and then the applied stress was released at the same strain rate until the stress on the specimens became zero. After this pre-stressing treatment, the specimens were cooled down to 4.2K for the measurement of the critical current I_c. The I_c-values were measured at the magnetic field H from 7 to 15 T by a 1 μV/cm criterion using a WM-5 magnet of the High Field Laboratory for Superconducting Materials, Tohoku University. The distance between current-probes was 25mm and that between voltage-ones was 10mm in this work. The former distance was regarded as the gauge length for the present specimens.
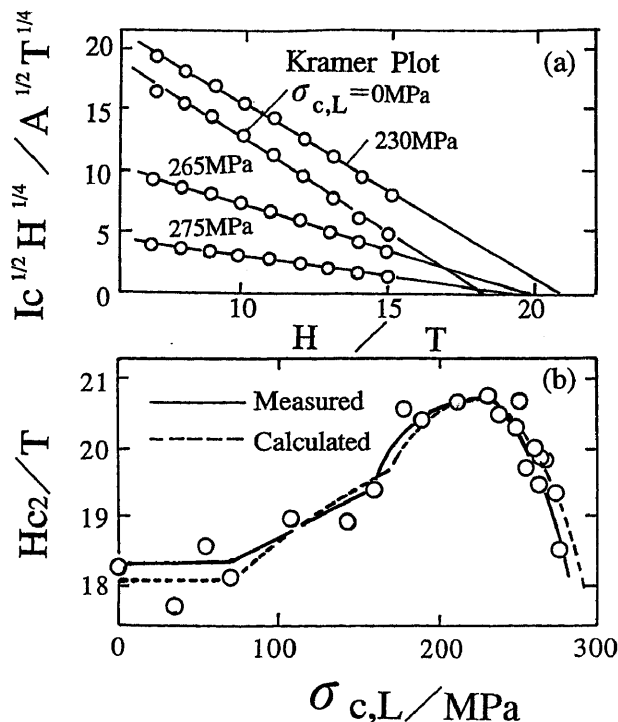
Figure 6 (a)Examples of the Kramer plot to estimate H_{c2}-values and (b)variations of H_{c2} as a function of $\sigma_{c,L}$. The broken curve in (b) shows the result of calculation by Eq.(1).
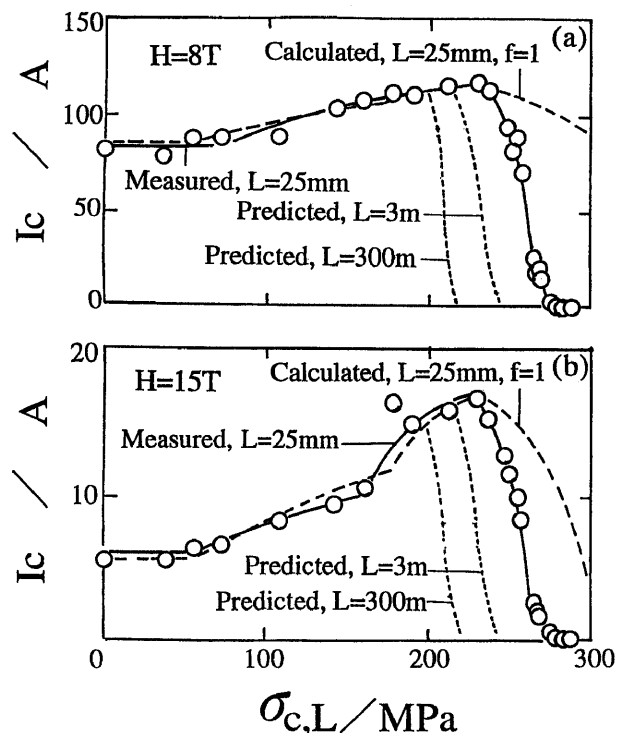
4. Application and Discussion

4-1 Variation of upper critical magnetic field due to the pre-stressing treatment

The H_{c2}-values are estimated by the Kramer plot[20], as typically shown in Fig.6(a). Figure 6(b) shows the variation of H_{c2}/H_{c2m} as a function of $\sigma_{c,L}$. The calculation results on $\sigma_{1,4,2K}$ for the present specimens indicate that the strain-free state at 4.2K is realized when $\sigma_{c,L} \approx 230$MPa. The maximum value of H_{c2}, H_{c2m}, which appears at $\sigma_{c,L} \approx 230$MPa was 20.8T. The dotted curves show the results of calculation by Eq.(1), describing well the experimental results, as shown in Fig.6(b).

4-2 Variation of critical current due to pre-stressing treatment

Figure 7 shows the variations of the measured values of I_c as a function of $\sigma_{c,L}$ for H=8 and 15T, respectively. The maximum critical current I_{cm}, which is realized at $\varepsilon_{1,4,2K}=0$ (strain-free, corresponding to $\sigma_{c,L} \approx 230$ MPa), was taken from the measured current of the specimen having the maximum $H_{c2}(=H_{c2m}:20.8T)$; $I_{cm}=116$A at 8T and $I_{cm}=16.5$A at 15T. The broken curves in Fig.7 show the results of calculation by Eq.(2), in which the measured values of H_{c2m} and the values of H_{c2} calculated by substituting $\varepsilon_{1,4,2K}$ and H_{c2m} into Eq.(1), together with H=8 and 15T, are substituted. These curves describe the variations of I_c arising from the strain effect for the assumed case where Nb_3Sn's are never broken even at high $\sigma_{c,L}$.

The following features are read from Fig.7: (i)The I_c increases with increasing $\sigma_{c,L}$, reaches maximum, and then decreases, through the change in $\sigma_{1,4,2K}$ (Fig.4(c)). (ii)At higher magnetic field(H=15T), the change in I_c becomes larger in comparison with that at lower field(H=8T), as expected from Eq.(2) (see also Fig.4(e) and (f)). (iii)For low $\sigma_{c,L}$, the measured values(solid curves) are in good agreement with the calculation results(broken curves), indicating that the change in I_c for low $\sigma_{c,L}$ is described well by the strain-effect given by Eq.(2). On the other hand, for high $\sigma_{c,L}$, the difference between the measured and calculated values of I_c/I_{cm} increases with increasing $\sigma_{c,L}$ due to the breakage of Nb_3Sn, as shown by the difference between the borken and solid curves.

In this way, the change in I_c as a function of $\sigma_{c,L}$ is affected both by the residual strain and breakage of Nb_3Sn. Summarizng the features mentioned above, the scaling law for the strain-effect on the critical current proposed by Ekin[10-12] gives a good description in the range of low $\sigma_{c,L}$ where no breakage of Nb_3Sn occurs. On the other hand, in the range of high $\sigma_{c,L}$ where some of the Nb_3Sn's are broken, the scaling law should be modified as to include the proportion of surviving Nb_3Sn's for the description of I_c, since only the surviving strained Nb_3Sn's transport the superconducting current.

Figure 7 Variations of I_c at H=(a)8T and (b)15T as a function of $\sigma_{c,L}$. The broken curves show the variations of I_c calculated by Eq.(2) which assumes no breakage of Nb_3Sn. The solid curves show the experimental variations for the gauge length L=25mm, being lower than the calculation results(broken curves) due to the breakage of Nb_3Sn in the range of high $\sigma_{c,L}$. The dotted curves show the variation of I_c for L=3 and 300m predicted by Eq.(3).
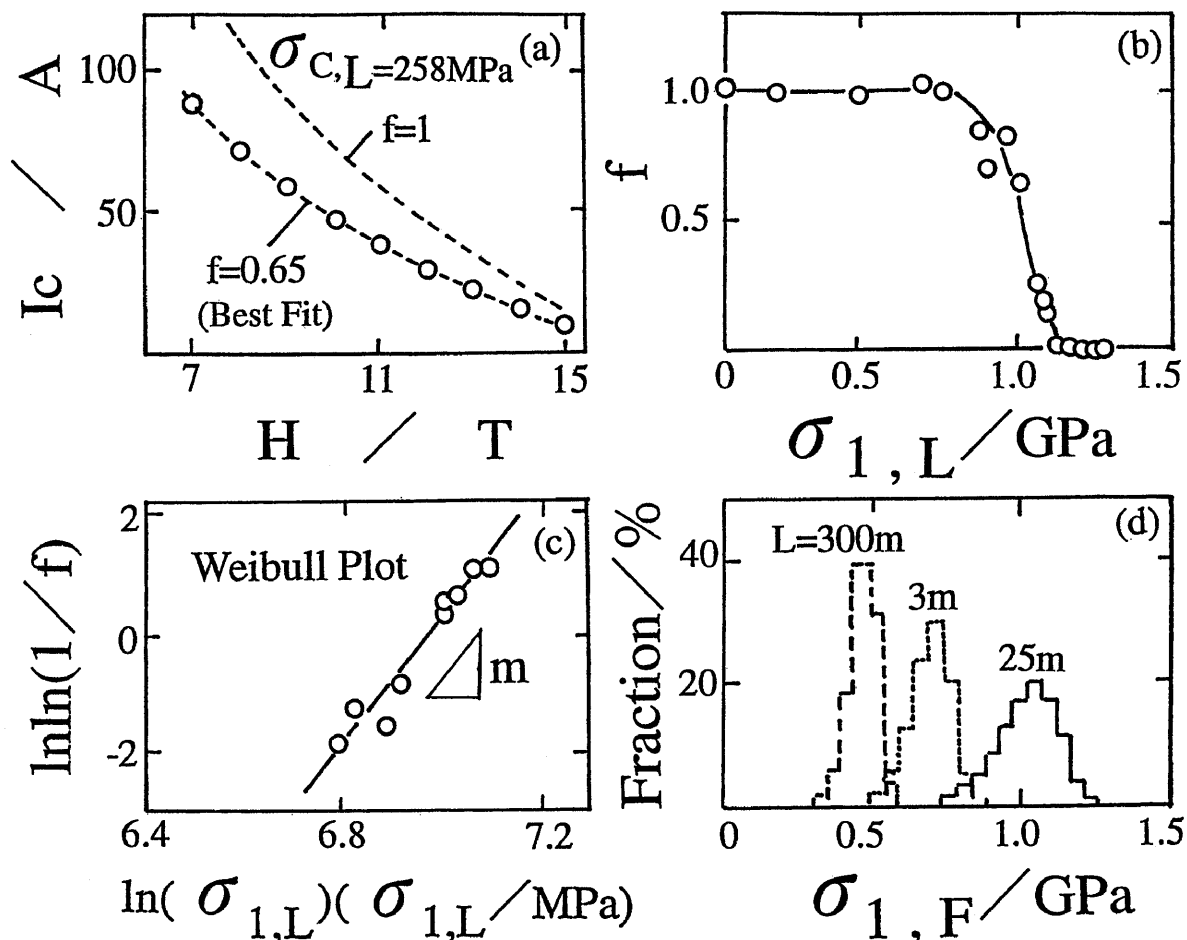
Figure 8 Estimation of strength distribution of Nb_3Sn. (a)An example of the curve-fitting to estimate f-value. (b)Estimated values of f, plotted against $\sigma_{1,L}$. (c)Values of $\ln\ln(1/f)$ plotted against $\ln(\sigma_{1,L})$. From the slope and intersection, the shape(m) and scale(σ_0) parameters in the Weibull distribution function were estimated. (d)Estimated distributions of strength of Nb_3Sn for L=25mm(=gauge length of the present specimens), 3m and 300m.

4-3 Estimation of strength and its scatter of Nb_3Sn

The proportioin of the surviving Nb_3Sn, f, is estimated as the best fit value to describe the experimental I_c-H relation expressed by Eq.(3). An example of the fitting is presented in Fig.8(a). Figure 8(b) shows the estimated values of f plotted against $\sigma_{1,L}$. It is read from Fig.8(b) that the strength of Nb_3Sn varies from 0.7 to 1.3GPa. The measured values of $\ln\ln(1/f)$ are plotted against $\ln(\sigma_{1,L})$, as shown in Fig.8(c). Then the values of m and σ_0 are estimated to be 12 and 0.8GPa(for L_0=1m) from the slope and intersection of the plot, respectively. The average strength calculated by Eq.(6) is 1.0 GPa. The scatter of the strength of the present Nb_3Sn(m=12) is larger than that of industrial metallic materials(m>30-50) but smaller than that of the high T_c $YBa_2Cu_3O_x$ in the silver sheath(m=3.4-6.4[21]). (3)The average strength of the Nb_3Sn is about 10 times higher than that of the high T_c oxides of $YBa_2Cu_3O_x$ and $Bi_2Sr_2Ca_2Cu_3O_y$ in the silver sheath[21,22].

4-4 Influence of length of specimens on the I_c-$\sigma_{c,L}$ relation

Substituting the estimated values of m and σ_0 into Eq.(4), the strength distributions of the Nb_3Sn can be calculated for any lengths. Figure 8(d) shows the distributions for L=25mm(gauge length of the present specimens), and for L=3 and 300m as examples. In this way, the strength of Nb_3Sn decreases with increasing L. The average strength for L=300m is reduced approximately to 0.4 times from that for L=25mm.

Judging from the tendency that the strength of long Nb_3Sn becomes very low, it might be speculated to a first sight that the permissible overall pre-stress on composite, below which the Nb_3Sn's are not broken (critical current can be retained), decreases seriously with increasing length. However, this speculation can be disputed; namely an extreme reduction in the permissible overall pre-stress does not occur, as shown below.

If we assume that the I_{cm} and H_{c2m} for long samples are not different from those for the present short samples(L=25 mm), the variation of I_c as a function of

$\sigma_{c,L}$ can be predicted for any length L and for any magnetic field H, by substituting the following values into Eq.(3) : I_{cm} and H_{c2m}(measured for L=25mm), H_{c2}(calculated by substituting H_{c2m} and $\varepsilon_{1,4.2K}$ into Eq.(1)), and f(calculated by sbustituting m, σ_0 and L_0=1m into Eq.(4)). The dotted curves in Fig.7 show the predicted variations in the range of high overall pre-stress for L=3 and 300m. Taking the case of L=300m, the reduction in I_c due to the breakage of Nb$_3$Sn occurs at $\sigma_{c,L} \approx 200$ MPa, while it occurs at $\sigma_{c,L} \approx 240$ MPa in case of L=25mm(indicated by the solid curve). Thus it is predicted that the permissible pre-stress on the present composite for L=300m is reduced by ≈ 20 % from that for L=25mm.

Although the reduction in strength of Nb$_3$Sn due to the extended length of specimens from 25mm to 300m is very large(about 60%), the reduction in permissible overall pre-stress on composite is relatively small (about 20%). The reason for this can be attributed to the situation that, even if L=300m, $\sigma_{1,L}$ does not reach the stress level necessary to cause breakage of Nb$_3$Sn(0.3-0.5GPa) until $\sigma_{c,L}$ becomes high(200-240MPa) as shown in Fig.4(b).

In the present work, an attempt to predict the I_c-values of pre-stressed long specimens from the data for short specimens is presented. Refinement of this method in addition to the accumulation of basic data will provide more accurate prediction of I_c-$\sigma_{c,L}$ relation and permissible pre-stress level for long composite wires, which will be utilized as a guide for practical handling.

5. Conclusions

An analytical method to describe the relation of the pre-stress applied on Nb$_3$Sn composite wire at room temperature to the upper critical magnetic field and critical current at 4.2K was presented. The application of this method revealed that (a)the upper critical magnetic field and critical current can be improved by application of appropriate pre-stress at room temperature through the decrease in residual strain in Nb$_3$Sn, (b)the strength distribution of Nb$_3$Sn in the present composite samples can be expressed by the Weibull distribution function with the shape parameter 12 and the scale parameter 0.80GPa for a standard length 1m, and (c)the permissible pre-stress on the composite, below which all Nb$_3$Sn filaments transport current without breakage, is reduced by ≈ 20% for long specimens of 300m in comparison with that for the short specimens of 25mm, while the

average strength of Nb$_3$Sn for 300m is reduced by ≈ 60% from that for 25mm.

1) D. S. Easton and R. E. Schwall : Appl. Phys. Lett. 39 (1976)216.
2) D. C. Larbalestier, J. W. McGraw and M. N. Wilson : IEEE Trans. Magn. MAG-13(1977)462.
3) T. Luhman, M. Suenaga, D. O. Welch and M. N. Kaiho : IEEE Trans. Magn. MAG-13(1977)699.
4) J. W. Ekin : Adv.Cryogen.Eng. 24(1978)306.
5) J. W. Ekin : IEEE Trans. Magn. MAG-15(1979)197.
6) S. Foner, R. Roberge, E. J. McNiff, Jr. and B. B. Schwarz : Appl. Phys. Lett. 34(1979)241.
7) G. Rupp : *Filamentary A15 Superconductors*, eds. M. Suenaga and A. F. Clark(Plenum,New York, 1980) p.155.
8) T. Luhman and D. O. Welch : ibid, p.171
9) D. M. Kroeger, D. S. Easton, C. C. Kock and A. Das-Gupta : ibid. p.205
10) J. W. Ekin : Cryogenics 20(1980)611.
11) J. W. Ekin : *Superconductor Materials Science: Metallurgy, Fabrication and Application*, eds. S. Foner and B. B. Schwarz (Plenum, New York, 1981) p.205
12) J. W. Ekin : *Composite Superconductors*, ed. K. Osamura (Marcel Dekker, New York, 1994) p.85.
13) S. Ochiai and K. Osamura : Acta Metall. 36(1988)1607.
14) S. Ochiai and K. Osamura : Acta Metall. 37(1989)2539.
15) S. Ochiai and K. Osamura : Cryogenics, 32(1992)584.
16) S. Ochiai, K. Osamura and K. Watanabe: J. Appl. Phys. 74(1993)440.
17) S. Ochiai, S. Nishino, M. Hojo, K. Osamura and K. Watanabe : Cryogenics, 35(1995)55.
18) S. Ochiai, S. Nishino, M. Hojo, K. Osamura and K. Watanabe: Teion-kogaku (Cryogenic Eng.), 30(1995)285. (in Japanese)
19) W. Weibull : J.Appl.Phys. 28(1951)293.
20) E. J. Kramer : J.Appl.Phys. 44(1973)1360.
21) S. Ochiai, K. Hayashi, A. Hosoda and K. Osamura : J. Mater. Sci. Lett. 10(1990)117.
22) S. Ochiai, K. Hayashi and K. Osamura : Cryogenics, 32 (1992)799.